



Contents lists available at SciVerse ScienceDirect

Bioorganic & Medicinal Chemistry Letters

journal homepage: www.elsevier.com/locate/bmcl

Discovery of new potential hits of *Plasmodium falciparum* enoyl-ACP reductase through ligand- and structure-based drug design approaches



Bruno J. Neves, Renata V. Bueno, Rodolpho C. Braga, Carolina H. Andrade*

Laboratório de Planejamento de Fármacos e Estudos de Metabolismo por Modelagem Molecular (LabMol), Faculdade de Farmácia, Universidade Federal de Goiás, Praça Universitária com 1a. Av., Goiânia, GO 74605-220, Brazil

ARTICLE INFO

Article history:

Received 2 August 2012

Revised 21 January 2013

Accepted 1 February 2013

Available online 13 February 2013

Keywords:

Enoyl-ACP reductase

Plasmodium falciparum

Drug design

QSAR

New inhibitors

ABSTRACT

We here report the discovery of novel *Plasmodium falciparum* enoyl-ACP reductase (PfENR) inhibitors as new antimalarial hits through ligand- and structure-based drug design approaches. We performed 2D and 3D QSAR studies on a set of rhodanine analogues using hologram QSAR (HQSAR), comparative molecular field analysis (CoMFA) and comparative molecular similarity indices analysis (CoMSIA) techniques. Statistical and satisfactory results were obtained for the best HQSAR (r^2 of 0.968 and q^2_{loo} of 0.751), CoMFA (r^2 of 0.955 and q^2_{loo} of 0.806) and CoMSIA (r^2 of 0.965 and q^2_{loo} of 0.659) models. The information gathered from the QSAR models guided us to design new PfENR inhibitors. Three new hits were predicted with potency in the submicromolar range and presented drug-like properties.

© 2013 Elsevier Ltd. All rights reserved.

Plasmodium falciparum (Pf) is the most lethal specie of *Plasmodium* genus infecting human beings, leading to malaria, a major growing threat to public health.^{1,2} According to the World Health Organization (WHO), about 220 million cases are diagnosed and approximately 1 million deaths per year, with over 2 billion people at risk for the disease.³ The resistance to known antimalarials and the lack of an effective vaccine have created an urgent need to discover new biologically active compounds.^{4,5} Potential biochemical targets for antimalarial drug discovery have been identified after the completed sequencing of the *P. falciparum* genome in 2002.^{6–8} The discovery of a type II fatty acid biosynthesis pathway (FAS II) in *Plasmodium falciparum* has opened new opportunities for malaria drug development.⁹ Fatty acids play a vital role in cells as metabolic precursors for biological membranes and energy storage.¹⁰ Many of FAS-II enzymes are involved in malarial viability. Particularly, the enoyl-ACP reductase (PfENR), which catalyzes the last reaction in each elongation circle, has been recognized and validated as an important drug target in *P. falciparum*.^{11,12}

An important strategy in designing new PfENR inhibitors is to identify key properties of the chemical structures related to their capability to induce biological response as a consequence of the PfENR inhibition. In last decades, quantitative structure–activity relationships (QSAR) have been successfully applied in the

development of relationships between structure properties of chemical substituent and their biological activities.^{13–15} Ligand-based QSAR approaches and receptor-based molecular docking studies are often complementary to each other and important in the development of new potent inhibitors.^{16–20}

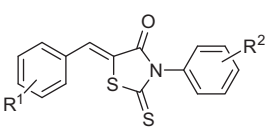
In this work, we report the identification of PfENR inhibitors as new antimalarial hits using an integration of ligand- and structure-based drug design approaches. To do so, we have employed a combination of a 2D-QSAR approach based on specialized molecular fragments, called hologram QSAR (HQSAR), 3D-QSAR using Comparative Molecular Field Analysis (CoMFA), and Comparative Similarity Indices Analysis (CoMSIA) methods for a series of rhodanine (2-thioxothiazolidin-4-one) analogs as PfENR inhibitors. In addition, molecular docking of the rhodanine analogs into the active site of PfENR was also carried out to identify the binding orientations and the protein–inhibitor interactions responsible for the observed activity. Hence, the information gathered by performing an integration of ligand- and structure-based approaches could help to better understand the structure–activity relationships and to design of new potent inhibitors of PfENR.

The QSAR studies were performed on a series of 36 rhodanine derivatives as inhibitors of PfENR, to which the in vitro enzymatic potency values (measured by IC_{50}) were collected from the literature.²¹ The IC_{50} (μM) values were expressed in negative logarithmic units, pIC_{50} ($-\log\text{IC}_{50}$) and used as dependent variables in QSAR analysis. The chemical structures and corresponding pIC_{50} are listed in Table 1. The IC_{50} values were obtained by the same

* Corresponding author.

E-mail address: carolina@farmacia.ufg.br (C. H. Andrade).

Table 1
Chemical structures and corresponding pIC₅₀ values of PfENR inhibitors



| Training set | | | |
|--------------|-----------------------------------------|----------------------------------|-------------------|
| Compound | R ¹ | R ² | pIC ₅₀ |
| 1 | 3,4-OH | 3,4-Me | 6.602 |
| 2 | 3,4-OH | 3-Cl | 6.097 |
| 3 | 3-OC ₂ H ₅ , 4-OH | 2-Me | 5.022 |
| 4 | 3-Br, 4-OH | 3-Me | 5.009 |
| 5 | 3-OC ₂ H ₅ , 4-OH | 4-Br | 4.857 |
| 6 | 3-NO ₂ , 4-Cl | 3-Cl | 4.730 |
| 7 | 3-Br, 4-OMe | 3-NO ₂ | 4.627 |
| 8 | 3-NO ₂ , 4-OH | 2,3-fused phenyl | 4.535 |
| 9 | 4-OH | 4-NO ₂ | 5.387 |
| 10 | 4-OH | 4-OC ₂ H ₅ | 5.081 |
| 11 | 4-OH | 3-F | 5.066 |
| 12 | 4-OH | H | 5.032 |
| 13 | 4-OH | 4-Br | 4.955 |
| 14 | 4-OH | 4-Cl | 4.676 |
| 15 | 4-OMe | 3-CF ₃ | 5.187 |
| 16 | 4-COOCH ₃ | 3-OH | 5.081 |
| 17 | 4-NO ₂ | 3-CF ₃ | 4.896 |
| 18 | 4-OMe | 3-OMe | 4.879 |
| 19 | 4-NO ₂ | 4-F | 4.833 |
| 20 | 4-CO ₂ H ₅ | 3-Cl | 4.724 |
| 21 | 4-COOH | 3-Cl | 5.060 |
| 22 | 4-COOH | 4-OH | 5.056 |
| 23 | 4-COOH | H | 5.041 |
| 24 | 4-COOH | 3-OMe | 5.009 |
| 25 | 3-OMe, 4-OH, 5-Cl | 4-NO ₂ | 5.004 |
| 26 | 3,4-OH, 5-Br | 3-CF ₃ | 5.004 |
| 27 | 2-COOH | 3-Cl | 4.921 |
| 28 | 2-COOH | 4-F | 4.573 |
| Test set | | | |
| 29 | 3,4-OH | 2,4-Me | 6.301 |
| 30 | 3,4-OH | 4-Cl | 5.102 |
| 31 | 3-OH, 4-OMe | 4-OMe | 5.004 |
| 32 | 3-OH | H | 5.066 |
| 33 | 3-OH | 3-OMe | 5.041 |
| 34 | 3-OMe | 4-COOMe | 4.565 |
| 35 | 4-OH | 3-OMe | 4.910 |
| 36 | 4-COOH | 2-F | 4.790 |

experimental conditions, and the pIC₅₀ values span a sufficiently wide range of three orders of magnitude. The compounds of both training and test sets were randomly selected subject to the constraint to ensure complete and representative coverage across the entire range of pIC₅₀ values. The models were externally validated using a test set with 8 compounds (Table 1) and were not included in the QSAR models development process.

SYBYL-X 1.2 (Tripos Inc., St. Louis, USA) was employed in QSAR modeling analyses, calculations and visualizations. All structures were built and energy minimized under the Tripos force field with a distance-dependent dielectric constant and Powell conjugate gradient method with a convergence criterion of 0.005 kcal/(mol Å). Partial atomic charges were calculated by the AM1-BCC method²² as implemented in QUACPAC.²³

HQSAR is a modern 2D-QSAR approach that uses molecular holograms as descriptors. HQSAR models can be affected by a number of parameters concerning hologram composition to get to models with the highest statistical parameters, such as hologram length (53–401), fragment size (2–5, 3–6, 4–7, 5–8, 6–9 and 7–10 atoms), and fragment distinction (atoms, A; bonds, B; connections, C; chirality, Ch; donor and acceptor, DA). Therefore, several combinations of these parameters were considered during

the HQSAR modeling runs. The patterns of fragment counts from the training set molecules were then related to the experimental potency values using the full cross-validated r^2 (q^2) partial least squares (PLS) leave-one-out (LOO) and leave-many-out (LMO) methods to assess model stability, robustness and statistical significance. The statistical results of HQSAR analyses for various fragment distinctions using the default fragment size (4–7) are presented in Table S1 (Supplementary data). The predictive ability of the models was assessed using the predictive correlation coefficient (r^2_{pred}) defined using Eq. 1.²⁴

$$r^2_{pred} = 1 - \left(\sum_{i=1}^N (y_i^{pred} - y_i)^2 \right) / \left(\sum_{i=1}^N (y_i - y_{mean}^{test})^2 \right) \quad (1)$$

where N is the number of compounds; y_i^{pred} is the predicted biological activity value of the i -th compound; y_i is the experimental value of biological activity; y_{mean}^{test} is the mean of the biological activity values of the test set compounds.

Although a measure of internal consistency, available in the forms of q^2 and r^2 , the most valuable test of a QSAR model is its ability to predict the activity of compounds not included in the training set. In this way, the predictive power of the best HQSAR model derived from the training set molecules (fragment distinction A/C/DA; fragment size 5–8, Table 2) was assessed by predicting the pIC₅₀ values for 8 test set molecules (compounds 29–36, Table 1), which were completely excluded from model generation.

The external validation results are listed in Table 3, and the graphic results for the experimental versus predicted activities of both compound sets (training and test sets) are displayed in Fig. S1A (Supplementary data). The predicted values fall closely to the experimental pIC₅₀ values, deviating by less than 0.508 log units. The excellent agreement between experimental and predicted pIC₅₀ values for the test set compounds indicates the robustness of the HQSAR model ($r^2_{pred} = 0.878$). Hence, in addition to good statistical quality and internal consistency, the best HQSAR model has shown high predictive power for novel PfENR inhibitors within this structural diversity.

Besides predicting the potency of untested compounds, HQSAR analyses also provide important hints about what molecular fragments are directly related to biological activity, which can be visualized through contribution maps. The colors of the red end of the spectrum (red, red orange, and orange) represent unfavorable or negative contribution to the activity, while the green end (yellow, green blue, and green) reflects otherwise; a positive contribution to the activity. Colored white are the atoms with intermediate contribution to the activity. The individual atomic contributions for the most (1) and least (34) potent compounds of the data set are shown in Figure 1. According to the contribution maps, the molecular fragments corresponding to the 5-benzylidene (R¹-phenyl ring) and the 2-thioxothiazolidin-4-one moieties are positive contributions to potency.

The main regions that negatively contribute to biological activity include the methoxy group linked to the R¹-phenyl ring and the R²-phenyl ring. These groups could be replaced by other substituents with different structural and physicochemical features with the aim to increase the affinity and potency of the compounds studied in this work.

Structural alignment is a crucial component in 3D-QSAR studies, since it affects the statistical results of CoMFA and CoMSIA. The accuracy and reliability of the model depends directly on the structural alignment rule.^{25–28} Therefore, three alignments were tested in this work, one receptor-dependent and two receptor-independent approaches. We used the rigid-body fit, ROCS^{29–31} ligand-based and structure-based alignments schemes, referred as

Download English Version:

<https://daneshyari.com/en/article/10596000>

Download Persian Version:

<https://daneshyari.com/article/10596000>

[Daneshyari.com](https://daneshyari.com)